Table V. Estimated Mixture Critical Points Using the Peng-Robinson Equation of State

T_c, K	P_c, MPa	x_{CO_2}
310.87	7.765	0.976
318.17	8.249	0.949
333.18	9.482	0.884

= 0.84 and σ_p = 6.91 which are also comparable to that found by Huron et al.

Figure 1 shows our data at all three temperatures, together with the best bubble point fit with the Peng-Robinson equation of state, with both temperature-dependent and temperature-independent binary interaction parameters. On the scale of this graph, the results obtained by using the Teja-Patel equation would be indistinguishable from those with the Peng-Robinson equation.

Also included in the figure and Table V are the mixture critical points estimated by using the Peng-Robinson equation of state, the binary interaction parameters appropriate to each temperature, and the computational technique described by Heidemann and Khalil (*5*), the Michelsen and Heidemann (*6*).

Finally, Figure 2 shows the departure of the predicted and experimental vapor-phase mole fractions of carbon dioxide. There we see that the compositional deviations are small, and that the Peng-Robinson predictions are generally lower than the measured vapor-phase mole fractions. Similarly, Figure 3 shows the departure of the predicted and experimental bubble point pressures. There we see that the predicted pressures are too low at low carbon dioxide mole fractions, and too high at the higher mole fractions, suggesting that the shape of the predicted phase envelope is not in complete agreement with experimental data. This is also evident from Figure 1.

Glossary

a, b, c	equation of state constants
k_{ij}	binary interaction coefficient
P	pressure
R	gas constant
T	temperature
V	molar volume
x	liquid-phase mole fraction
y	vapor-phase mole fraction

Registry No. CO_2, 124-38-9; cyclopentane, 287-92-3.

Literature Cited

(1) Behrens, P. K.; Sandler, S. I. *J. Chem. Eng. Data* **1983**, *28*, 52.
(2) Peng, D.-Y.; Robinson, D. B. *Ind. Eng. Chem. Fundam.* **1978**, *15*, 59.
(3) Patel, N. C.; Teja, A. S. *Chem. Eng. Sci.* **1982**, *27*, 463.
(4) Huron, M.-J.; Durou, G.-N., and Vidal, J. *Fluid Phase Equilib.* **1977**, *1*, 247.
(5) Heidemann, R. A.; Khalil, A. M. *AIChE J.* **1980**, *26*, 769.
(6) Michelsen, M. L.; Heidemann, R. A. *AIChE J.* **1981**, *27*, 521.

Received for review November 26, 1984. Accepted June 21, 1985. We are pleased to acknowledge the financial support of the Chevron Oil Field Research Co., the Mobil Foundation, and the Department of Chemcial Engineering at the University of Delaware for this work.

Phase Equilibria for Water–Decane–Propan-1-ol and Water–Butan-1-ol at 20 °C, Including Density and Refractive Index

Eric G. Mahers[†] and Richard A. Dawe*

Mineral Resources Engineering Department, Imperial College, London SW7 2AZ, U.K.

Compositions along the binodal curve of the system water–decane–propan-1-ol at 20 °C have been determined gravimetrically, and characterized by measuring the refractive index and density along the binodal curve. Tie lines were determined from these measurements. The refractive index and density of the miscible system decane–propan-1-ol and the partially miscible system water–butan-1-ol are also reported.

Introduction

Density and refractive index measurements are commonly used for analysis of binary and ternary mixtures. In studies of displacements in porous media modelling oil reservoir behavior, a miscible binary system, decane–propan-1-ol, and a partially miscible ternary system, water–decane–propan-1-ol, have been used (*1*, *2*).

Experimental Section and Results

Components were purchased in their highest commercial purity and used without further purification. The decane was supplied by Koch-Light Ltd., the propan-1-ol and butan-1-ol by British Drug Houses (AnalaR grade), and the water was singly distilled.

Fluid densities were measured to ±0.1 kg m^{-3} with a $4^1/_2$-digit Anton Parr Model DMA 46 digital density meter, calibrated with water and air according to the maker's instructions. The refractive indices were measured to a precision of $\pm 4 \times 10^{-5}$ by a Bellingham and Stanley Abbè "60" refractometer, Model "high accuracy 60/ED". The refractive indices were measured at the sodium doublet line 589.3 nm and the instrument calibrated with a silica standard. Both instruments were thermostatically controlled at 20 ± 0.05 °C.

Water–Decane–Propan-1-ol System. The phase diagram of the water–decane–propan-1-ol system was determined as follows. The compositions along the binodal curve were determined gravimetrically. For the water-rich side of the system, 10 mL of water were placed in a flask held on an electronic balance measuring to 0.01 g and the mass noted. A drop of decane was added, thus forming a two-phase mixture and the mass noted again. Sufficient propan-1-ol was added to dissolve the decane into the aqueous phase, the mass added noted, and the composition calculated. More decane was added to the system, followed by propan-1-ol to again reach miscibility. The decane-rich compositions were determined similarly but starting with 10 mL of decane and adding water and then propan-1-ol.

[†] Now with Unilever Research, Merseyside, U.K.

0021-9568/86/1731-0028$01.50/0 © 1986 American Chemical Society

Table I. Compositions along the Binodal Curve for Water-Decane-Propan-1-ol at 20 °C

mass fraction			mass fraction		
water	decane	propan-1-ol	water	decane	propan-1-ol
0.605	0.002	0.393	0.176	0.109	0.715
0.579	0.002	0.419	0.172	0.118	0.710
0.572	0.003	0.425	0.169	0.117	0.714
0.541	0.004	0.455	0.159	0.132	0.709
0.536	0.004	0.460	0.154	0.137	0.709
0.532	0.005	0.463	0.145	0.150	0.705
0.527	0.006	0.467	0.143	0.155	0.702
0.519	0.005	0.476	0.138	0.157	0.705
0.508	0.007	0.485	0.129	0.178	0.693
0.495	0.008	0.497	0.123	0.184	0.693
0.485	0.009	0.506	0.118	0.198	0.684
0.476	0.010	0.514	0.114	0.198	0.688
0.466	0.010	0.524	0.109	0.220	0.671
0.465	0.009	0.526	0.099	0.245	0.656
0.459	0.011	0.530	0.094	0.248	0.658
0.455	0.013	0.542	0.091	0.269	0.640
0.417	0.017	0.566	0.085	0.293	0.622
0.411	0.015	0.574	0.079	0.312	0.609
0.401	0.020	0.579	0.075	0.332	0.593
0.392	0.022	0.586	0.071	0.348	0.581
0.384	0.023	0.593	0.070	0.351	0.579
0.373	0.024	0.603	0.065	0.378	0.557
0.357	0.029	0.614	0.063	0.375	0.562
0.330	0.030	0.640	0.061	0.402	0.537
0.323	0.033	0.644	0.056	0.431	0.513
0.301	0.038	0.661	0.051	0.465	0.484
0.287	0.040	0.673	0.048	0.490	0.462
0.282	0.042	0.676	0.045	0.499	0.456
0.266	0.047	0.687	0.043	0.524	0.433
0.254	0.054	0.692	0.038	0.569	0.393
0.241	0.061	0.698	0.032	0.615	0.353
0.238	0.059	0.703	0.029	0.619	0.352
0.229	0.068	0.703	0.027	0.659	0.314
0.217	0.078	0.705	0.022	0.703	0.275
0.217	0.074	0.709	0.017	0.747	0.236
0.207	0.086	0.707	0.015	0.768	0.217
0.196	0.094	0.710	0.008	0.849	0.143
0.193	0.098	0.709	0.005	0.886	0.109
0.179	0.107	0.714	0.004	0.960	0.036

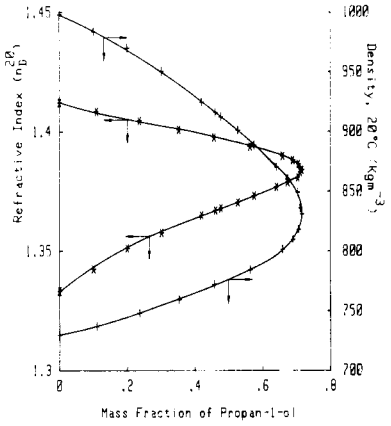

Figure 1. Refractive index and density, both at 20 °C, along the binodal curve of water–decane–propan-1-ol.

The data are given in Table I.

The binodal curve was characterized by measuring the refractive index and density of mixtures made up with compositions along the binodal. These data are given in Table II and plotted against the mass fraction of propan-1-ol in Figure 1.

The tie lines were determined by making up mixtures with overall compositions lying within the two-phase region and, after being shaken well and allowed to settle, samples were carefully taken from each phase and the fraction of propan-1-ol calculated from the refractive index and density curves. The raw data are given in Table III.

Table II. Refractive Index (n^{20}_D) Relative to Air and Density (20 °C) along the Binodal Curve for Water-Decane-Propan-1-ol

mass fraction				density,
water	decane	propan-1-ol	n^{20}_D	kg m^{-3}
1.000	0.000	0.000	1.333 27	998.1
0.900	0.000	0.100	1.342 50	983.6
0.800	0.000	0.200	1.351 22	969.9
0.699	0.000	0.301	1.357 75	950.3
0.579	0.002	0.419	1.365 04	924.5
0.536	0.004	0.460	1.367 12	915.8
0.519	0.005	0.476	1.368 03	912.3
0.465	0.009	0.526	1.370 50	900.9
0.411	0.015	0.574	1.373 14	888.4
0.330	0.030	0.640	1.376 84	870.0
0.287	0.040	0.673	1.378 76	860.2
0.238	0.059	0.703	1.380 84	849.1
0.196	0.094	0.710	1.383 05	836.1
0.176	0.109	0.715	1.383 94	831.1
0.138	0.157	0.705	1.386 39	818.0
0.114	0.198	0.688	1.388 01	809.6
0.094	0.248	0.658	1.389 81	801.3
0.063	0.375	0.562	1.393 76	784.2
0.045	0.499	0.456	1.397 59	772.2
0.029	0.619	0.352	1.400 79	759.5
0.017	0.747	0.236	1.404 49	748.0
0.005	0.886	0.109	1.408 48	737.0
0.000	1.000	0.000	1.412 13	730.0

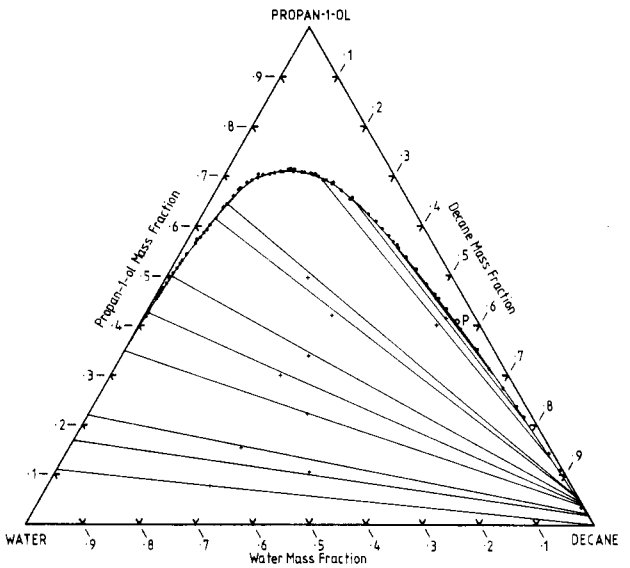

Figure 2. Binodal curve and tie lines of the system water–decane–propan-1-ol at 20 °C. The plait point P is 0.55 decane, 0.41 propan-1-ol mass fraction. + = the initial immiscible mixtures from which the tie lines were determined.

The binodal curve and the tie lines are shown on the triangular diagram, Figure 2, where the compositions are plotted as mass fractions. The + marks are the compositions of the initial immiscible mixtures from which the tie lines were determined; the tie lines have been drawn from the measured separated samples. The composition of the plait point, p, is 0.55 decane, 0.41 propan-1-ol mass fraction.

Decane–Propan-1-ol System. This system is miscible. Mixtures of decane and propan-1-ol were made up and characterized by refractive index, n^{20}_D, and density, ρ. The data are given in Table IV and shown in Figure 3, and can be represented by

$$n^{20}_D = 2.51653 \times 10^{-3} m_p^2 - 2.92095 \times 10^{-2} m_p + 1.41204 \quad (1)$$

with σ, the standard deviation, of 7×10^{-5}, and

$$\rho/\text{kg m}^{-3} = 16.1312 m_p^2 + 58.2143 m_p + 729.629 \quad (2)$$

Table III. Determination of the Tie Lines for Water-Decane-Propan-1-ol

n^{20}_D[a]		density,[b] kg m^{-3}		composition[c]					
				aqueous phase			oleic phase		
aqueous	oleic	aqueous	oleic	water	decane	propan-1-ol	water	decane	propan-1-ol
1.343 50	1.411 92	982.4	729.4	0.890	0.000	0.110	0.000	1.000	0.000
1.349 13	1.411 26	973.5	730.7	0.830	0.000	0.170	0.005	0.975	0.020
1.352 41	1.411 62	967.1	731.2	0.780	0.000	0.220	0.005	0.970	0.025
1.360 71	1.410 63	940.2	731.9	0.650	0.000	0.350	0.005	0.955	0.040
1.365 01	1.410 74	923.9	730.7	0.570	0.005	0.425	0.005	0.950	0.045
1.368 98	1.410 50	906.5	732.3	0.492	0.008	0.500	0.005	0.945	0.050
1.375 29	1.410 40	887.7	732.4	0.360	0.025	0.615	0.005	0.940	0.055
1.376 87	1.409 97	868.8	732.9	0.320	0.035	0.645	0.005	0.935	0.060
1.387 03	1.408 64	814.9	736.6	0.135	0.165	0.700	0.005	0.885	0.110
1.390 23	1.407 11	798.9	740.4	0.095	0.255	0.650	0.010	0.835	0.155
1.393 51	1.404 55	784.6	747.3	0.065	0.365	0.570	0.020	0.745	0.235

[a] Refractive index. [b] 20 °C. [c] In mass fraction.

Table IV. Refractive Index (n^{20}_D) Relative to Air and Density (20 °C) for Mixtures of Decane and Propan-1-ol

mass fraction		n^{20}_D	density, kg m^{-3}
decane	propan-1-ol		
0.000	1.000	1.385 32	803.9
0.111	0.889	1.388 04	794.1
0.201	0.799	1.390 30	786.6
0.317	0.683	1.393 37	776.8
0.363	0.637	1.394 49	773.3
0.504	0.496	1.398 18	762.6
0.623	0.377	1.401 32	753.9
0.678	0.322	1.402 85	750.1
0.800	0.200	1.406 36	741.8
0.901	0.099	1.409 03	735.1
1.000	0.000	1.412 15	730.0

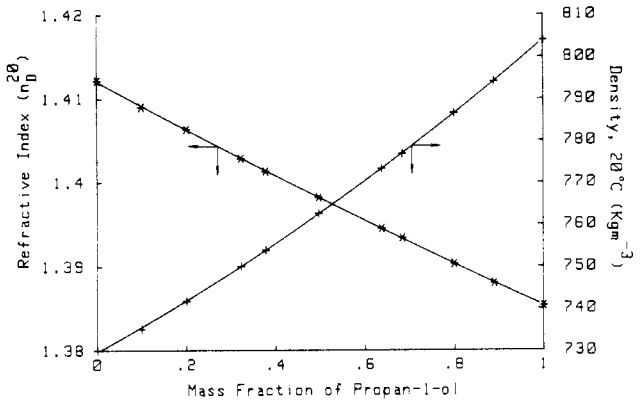

Figure 3. Refractive index and density, both at 20 °C, for decane–propan-1-ol.

with σ of 0.2 kg m^{-3}.

Water–Butan-1-ol. This system is partially miscible. The data are given in Table V and Figure 4 and can be represented by the following equations:

for $0 \leq m_w \leq 0.2$

$$n^{20}_D = -5.8655 \times 10^{-2} m_w^2 - 3.1724 \times 10^{-2} m_w + 1.39964 \quad (3)$$

with σ of 4×10^{-5}, and

$$\rho/\text{kg m}^{-3} = 188.515 m_w + 810.382 \quad (4)$$

with σ of 0.26 kg m^{-3};

for $0.923 \leq m_w \leq 1$

$$n^{20}_D = -1.03744 \times 10^{-1} m_w + 1.43701 \quad (5)$$

with σ of 6×10^{-5}, and

$$\rho/\text{kg m}^{-3} = 141.615 m_w + 856.571 \quad (6)$$

Table V. Refractive Index (n^{20}_D) Relative to Air and Density (20 °C) for Mixtures of Water and Butan-1-ol[a]

mass fraction		n^{20}_D	density, kg m^{-3}
water	butan-1-ol		
0.000	1.000	1.399 56	809.9
0.017	0.983	1.399 15	813.5
0.003	0.967	1.398 59	816.9
0.068	0.932	1.397 19	823.7
0.109	0.891	1.395 49	831.0
0.137	0.863	1.394 15	836.1
0.172	0.828	1.392 46	842.7
0.190	0.810	1.391 49	846.2
0.200*	0.800*	1.390 97	848.0*
0.923*	0.077*	1.341 32	987.4*
0.930	0.070	1.340 55	988.3
0.933	0.067	1.340 13	988.7
0.943	0.057	1.339 17	990.1
0.967	0.033	1.336 70	993.3
0.979	0.021	1.335 40	994.9
0.989	0.011	1.334 34	996.9
1.000	0.000	1.333 35	998.3

[a] The asterisk denotes equilibrium composition at two-phase boundary.

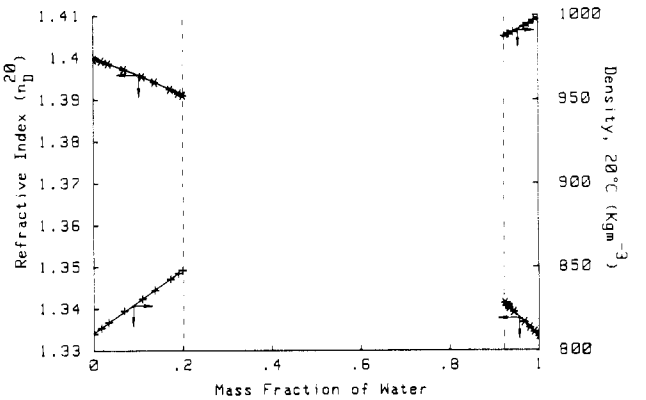

Figure 4. Refractive index and density, both at 20 °C, for water–butan-1-ol.

with σ of 0.17 kg m^{-3}.

Glossary

n^{20}_D	refractive index relative to air measured at 589.3 nm and 20 °C, ±0.00004
ρ	density at 20 °C, ±0.1 kg m^{-3}
m_p, m_d, m_w	mass fraction of propan-1-ol, decane, water

Registry No. Butan-1-ol, 71-36-3; propan-1-ol, 71-23-8; decane, 124-18-5.

Literature Cited

(1) Mahers, E. G. Ph.D. Thesis, University of London (Imperial College), November 1983.

(2) Mahers, E. G.; Dawe, R. A. "SPE/DOE Fourth Symposium on Enhanced Oil Recovery", Tulsa, OK, April 1984, Society Petroleum Engineers preprint 12679. *Soc. Pet. Eng. J.*, in press.

Received for review November 20, 1984. Accepted July 23, 1985. We thank the Science and Engineering Research Council, U.K., for support.

Densities of Aqueous Lithium, Sodium, and Potassium Hydroxides from 25 to 75 °C at 1 atm

Thelma M. Herrington,* Alan D. Pethybridge, and Michael G. Roffey

Department of Chemistry, University of Reading, Whiteknights, Reading RG6 2AD, England

A weight dilatometer has been used to measure the densities of aqueous solutions of lithium, sodium, and potassium hydroxides up to 3 *m* at 10 °C intervals in the range 25–75 °C at 1.013 bar. The precision of the densities is ±1 × 10^{-5} g cm^{-3}. The data are compared with literature values where applicable.

Introduction

In the conversion of fossil and nuclear energy to electricity high-temperature solution-phase thermodynamic data are required to improve plant reliability. For example, most corrosion problems in boiler water circuits arise where the solution can concentrate; the compositions of these concentrated solutions can only be obtained from thermochemical data. In order to obtain density data at high temperatures it is necessary to have a good knowledge of the density at lower temperatures. Currently there is a great lack of solution density data on alkalis at temperatures other than room temperature. In this work we have been interested in developing a technique which can be used to obtain data at atmospheric pressure and that can be relatively easily adapted to measuring densities under pressure at high temperatures. This technique is used to provide the basic low-temperature data for the high-temperature study.

Experimental Section

Materials. The alkali hydroxides used were AR grade. Carbonate-free solutions were prepared by precipitation of carbonate using the method described by Vögel (*1*). The carbonate-free hydroxide solutions were then stored under nitrogen in blacked-out plastic containers until use. The potassium hydrogen phthalate used for standardization was recrystallized 3 times from conductivity water after a hot filtration; it was then dried in the vacuum oven and stored under vacuum until use. All solutions were prepared by using demineralized water which was first distilled and then passed through a nuclear-grade mixed bed in-exchange resin, followed by a filter column until its conductivity was less than 0.05 μS cm^{-1}. All mercury used was recovered and cleaned by a four-stage process, dried by passing air through it in contact with AR grade acetone, and stored under nitrogen in plastic containers until use.

All solutions were degassed by boiling under reduced pressure for $^1/_2$ h before standardization. The hydroxide solutions were standarized by titration against weighed portions of a potassium hydrogen phthalate solution, which had been made up by weight, using a Metrohm 636 Titroprocessor in conjunction with a Metrohm E635 Dosimat unit. This procedure gave a reproducibility of better than 0.005%.

Table I. Density of Water

T/K	ρ_0/g cm^{-3}	T/K	ρ_0/g cm^{-3}
298.15	0.997 048	328.15	0.985 696
308.15	0.994 035	338.15	0.980 553
318.15	0.990 216	348.15	0.974 844

Solutions were made up by weight and buoyancy corrections applied; the air density at the time of weighing was calculated from tables (*2*). Two balances were used during this work: first, a Stanton SM12 double pan balance, used in conjunction with a set of National Physical Laboratory (NPL) calibration stainless steel weights, and second, a Sartorius 2004 MP electronic balance. Both balances gave a precision of ±2 × 10^{-5} g and operated over a range of 0–160 g. The two balances agreed to within ±1 × 10^{-5} g on a given weight.

Dilatometer. The dilatometer used was similar in design to the weight dilatometer of Gibson and Loeffler (*3*), but was made of titanium. The opening for filling the dilatometer was made as narrow as possible and the flange was sealed by a flat plate clamped against a silicone rubber seating. The principle of operation is that mercury is diplaced through a capillary from the dilatometer and collected in a preweighed pot. The advantage of this method is that it allows a large number of measurements to be made over several temperatures without refilling the dilatometer, to give a precision of ±1 × 10^{-5} g cm^{-3}. Values for the density of water were taken from Kell (*4*) (Table I) and for the density of mercury from ref *2*. The temperature of the water thermostat was monitored with an NPL calibrated platinum resistance thermometer, in conjunction with an Automatic Systems Laboratories precision ac double transformer ratio bridge (Model H6), to ±1 × 10^{-3} K. Temperature control was better than ±2 × 10^{-3} K.

Results and Discussion

Values for the density of each electrolyte were obtained at 10-deg intervals between 25 and 75 °C, and over a 0.5–3 *m* concentration range. Measurements were not carried out below 0.5 *m* as a precision of ±1 × 10^{-5} g cm^{-3} in the density gives an error of ±0.02 cm^3 mol^{-1} in the apparent molar volume at 0.5 *m* but ±0.1 cm^3 mol^{-1} at 0.1 *m*. The results for lithium hydroxide, sodium hydroxide, and potassium hydroxide are given in Tables II–IV. The apparent molar volume of each solution was calculated from these data by using eq 1 (see Glossary at end of paper).

$$^{\phi}V = \frac{1}{m}\left(\frac{1}{\rho} - \frac{1}{\rho_0}\right) + \frac{M_2}{\rho} \qquad (1)$$

0021-9568/86/1731-0031$01.50/0 © 1986 American Chemical Society